The Journal of Experimental Biology 210, 553-560
Published by The Company of Biologists 2007
doi:10.1242/jeb.02682

Adhesive recruitment by the viscous capture threads of araneoid orb-weaving spiders

Brent D. Opell* and Mary L. Hendricks
Department of Biological Sciences, Virginia Polytechnic Institute and State University, Blacksburg, VA 24061, USA
*Author for correspondence (e-mail: bopell@vt.edu)

Accepted 5 December 2006

Summary

The sticky prey capture threads of orb-webs are critical to web performance. By retaining insects that strike the web, these spirally arrayed threads allow a spider time to locate and subdue prey. The viscous capture threads spun by modern orb-weaving spiders of the Araneoidea clade replaced the dry, fuzzy cribellar capture threads of the Deinopoidea and feature regularly spaced moist, adhesive droplets. The stickiness of a cribellar thread is limited by its tendency to peel from a surface after the adhesion generated at the edges of contact is exceeded. In this study we test the hypothesis that viscous thread overcomes this limitation by implementing a suspension bridge mechanism (SBM) that recruits the adhesion of multiple thread droplets. We do so by using contact plates of four widths to measure the stickiness of six species' viscous threads whose profiles range from small, closely spaced droplets to large, widely spaced droplets. The increased stickiness registered by an increased number of thread droplets supports the operation of a SBM. However, the accompanying decrease in mean per droplet adhesion shows that droplets interior to the edges of thread contact contribute successively less adhesion. Models developed from these data suggest that the suspension bridge mechanism is limited to a span of approximately 12 droplets.

Key words: adhesive mechanism, capture thread, orb-web.

Introduction

Spider orb-webs represent the confluence of intricate architecture (Craig, 1987a,b; Craig, 2003; Eberhard, 1990) and natural materials that have optimal mechanical properties (Denny, 1976; Guerette et al., 1996; Gosline et al., 1999; Gosline et al., 2002; Hayashi and Lewis, 2000; Craig, 2003; Hayashi et al., 2004; Blackledge and Hayashi, 2006a; Vollrath and Porter, 2006a; Vollrath and Porter, 2006b). The web's non-sticky, supporting threads effectively absorb the forces of prey strikes and its sticky, spirally arrayed capture threads retain insects long enough for a spider to subdue them (Chacón and Eberhard, 1980). The first modern orb-weaving spiders (Araneoidea clade) appeared in the Cretaceous (Selden, 1989; Peñalver et al., 2006) and have since spun viscous capture threads comprised of fibers covered by regularly spaced, sticky droplets (Fig. 1). These composite threads are spun from the spigots of two adjacent silk glands (Foelix, 1996): flagelliform glands that produce a pair of supporting axial fibers and aggregate glands that coat these fibers with a complex viscous, aqueous solution (Gosline et al., 1984; Peters, 1986; Peters, 1995; Vollrath et al., 1990). Soon after threads are spun, this solution forms regularly spaced droplets, whose size and spacing are probably determined by the amount of material deposited, the axial fibers' diameters, and the solution's viscosity. The size of the glycoprotein granules that coalesce inside each droplet and contribute to thread adhesion may also affect droplet size (Vollrath and Tillinghast, 1991). Hydrophilic compounds in the viscous fluid maintain droplet size by attracting atmospheric moisture and preventing droplets from drying (Townly, 1990; Townly et al., 1991).

These viscous droplets replaced the minute, dry protein fibrils that form torus shaped puffs around the axial fibers of cribellar capture threads (Peters, 1984; Peters, 1986; Opell, 1994a; Opell, 1997a), the plesiomorphic capture threads spun by members of the Deinopoidea clade, the sister group of the of the Araneoidea (Coddington, 1986; Coddington, 1989; Griswold et al., 1998; Garb et al., 2006). The Araneoidea now far outnumber the Deinopoidea, comprising over 27% of the 39 490 living spider species (Platnick, 2006). Araneoid origin was associated with three changes that enhance orb web performance and may have contributed to the success of this lineage (Bond and Opell, 1998). The web's ability to intercept prey was enhanced by a transition from horizontal to vertical web orientation (Chacón and Eberhard, 1980; Eberhard, 1989) and by the reduced visibility of viscous capture thread (Craig and Berhard, 1990; Craig et al., 1994; Zschokke, 2002). The web's ability to retain insects that strike it was improved by the enhanced stickiness of viscous thread (Opell, 1997b; Opell, 1998; Opell, 1999).

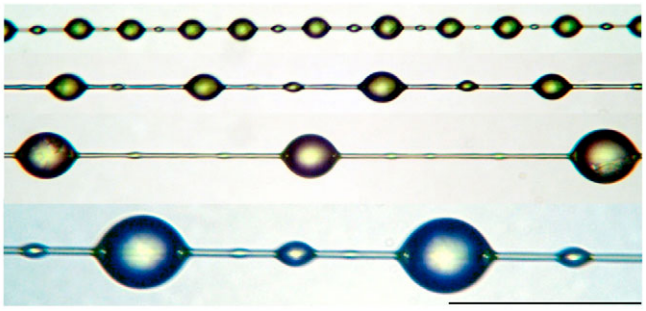

Fig. 1. Viscous capture threads of (from top to bottom) *Leucauge venusta*, *Metepeira labyrinthea*, *Araneus pegnia*, and *Araneus marmoreus*. Scale bar, 100 μm.

The operation of cribellar and viscous capture threads differs in at least four ways: (1) the adhesion achieved per volume of thread material; (2) the scale at which a thread interacts with a surface; (3) the efficiency with which adhesive forces are transferred to the thread's axial fibers; and (4) the ability of a thread span to recruit adhesion from interior regions of contact. Relative to the volume of material that they contain, viscous threads achieves an average of 13 times more adhesion than cribellar threads (Opell, 1998). The surfaces of cribellar threads are formed of thousands of fibrils, each with a diameter of around 20 nm (Hawthorn and Opell, 2002; Hawthorn and Opell, 2003; Opell, 1994a). These fibrils implement mechanical interlock to snag on insect setae and irregular surfaces (Opell, 1994b) and additional mechanisms to adhere to smooth surfaces. Fibrils of all but the most primitive cribellar threads feature regularly spaced, 35 nm diameter nodes that establish as many as 170 points of interaction with each μm^2 of surface they contact (Hawthorn and Opell, 2003). At low relative humidity each of these nodes generates van der Waals forces, but at a relative humidity of 45% or greater they generate stronger capillary forces (Hawthorn and Opell, 2003). In contrast, viscous threads typically have 30 or fewer droplets per mm and mean droplet dimensions of 10 μm or greater (Craig, 1987a; Opell, 1998). Thus, cribellar thread generates adhesion at many small, diffuse points of contact, whereas viscous thread generates adhesion at a few large points of contact.

As cribellar thread establishes a large number of very small points of contact over a wide area, the force vectors of the fibrils are not aligned and fibrils pull on one another as force is applied to axial fibers. Thus, the adhesion generated at these points is probably not effectively summed and transferred to the thread's axial fibers. In contrast, viscous thread generates adhesion at a much smaller number of in-line droplets and appears better equipped to effectively transfer this force to the axial fibers. A striking feature of cribellar thread is its inability to generate increased adhesion with increased length of contact. When cribellar threads were anchored at their ends and pulled away from contacting surfaces of two or four different widths, no significant increase in stickiness was observed as plate width increased (Hawthorn and Opell, 2003) (B.D.O., unpublished). Thus, it appears that useful adhesion is generated only in narrow bands at the outer edges of a cribellar thread's contact with a surface. When this adhesion is exceeded, the more central regions of the thread peel free from the contacting surface without adding substantially to the thread's adhesion.

The lower extensibility of cribellar thread when compared with viscous thread (Opell and Bond, 2000; Opell and Bond, 2001) may contribute to the tendency of cribellar thread adhesion to fail in this way. If a cribellar thread achieves only a small incident angle with a contacting surface, then most of the force applied to the thread would be perpendicular to the surface to which it is attached and little of the force would be directed along the thread in a manner favoring the recruitment of adhesion from more interior regions of thread contact (Fig. 2). In contrast, the greater extensibility of viscous threads should combine with the plasticity of their regularly spaced, viscoelastic droplets to produce a highly extensible system capable of generating a greater angle of incidence under a load (Fig. 2). This configuration would transfer more force along the thread's axial lines, thereby recruiting adhesion generated by inner droplets.

We hypothesize that the ability of viscous thread to generate greater adhesion relative to its material volume (Opell, 1998) is due in part to its ability to implement a suspension bridge mechanism (SBM) that effectively recruits the adhesion of multiple droplets (Fig. 2). Just as each of the vertical cables of a suspension bridge transfer force to the larger, upper horizontal cable, we believe that the adhesive forces generated by viscous droplets are transferred to a thread's axial fibers. This mechanism is established when, after making firm contact with a surface, droplets stretch as force is exerted on the thread, transferring this force to elastic

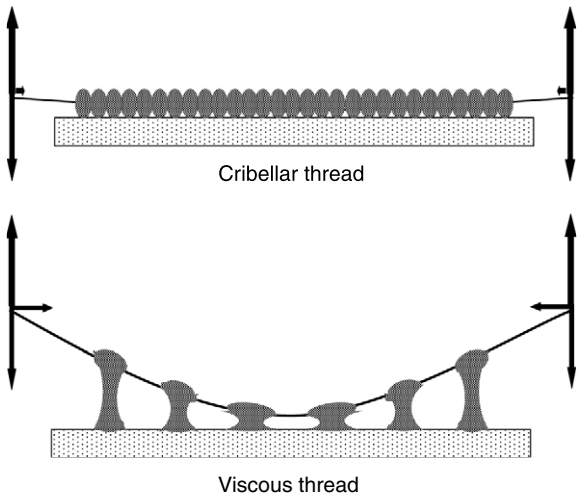

Fig. 2. Models of cribellar and viscous capture threads under a load showing how the greater elasticity of the axial fibers of viscous threads and the plasticity of viscous droplets allow viscous threads to form more acute angles with a contacting surface and, thereby, to direct a higher proportion of force perpendicular to a force pulling on the thread.

axial fibers. When a viscous thread under a load is observed with a dissecting microscope, its configuration is consistent with the operation of the hypothesized SBM. Additionally, the axial fibers of viscous threads appear particularly well adapted to operate in this way. Although the axial fibers of cribellar and viscous capture threads are homologous (Garb et al., 2006), those of viscous thread are more extensible (Blackledge and Hayashi, 2006b). The hypothesized SBM would increase thread stickiness both by increasing the number of droplets that contribute to the stickiness of a thread span and by resisting the edge-to-center peeling that appears to limit the stickiness of cribellar thread.

We test this hypothesis by measuring the stickiness of threads spun by six Araneoidea species, whose droplet profiles range from small, closely spaced droplets to large, widely spaced droplets. We measure the stickiness of each species' threads with contact plates of four widths to alter the number of droplets that contribute to the stickiness of a thread span. The SBM predicts that thread stickiness should increase as the length of thread contact increases. However, a thread's droplet profile may limit the effectiveness of the SBM, as internal droplets that are farthest removed from the edges of thread contact may contribute little to overall thread adhesion. To better understand this system, we use the 24 stickiness values generated in this study (mean values of four plate widths for each of six species' threads) to develop a model of thread performance that incorporates droplet spacing, contact plate width, and the adhesion of individual droplets.

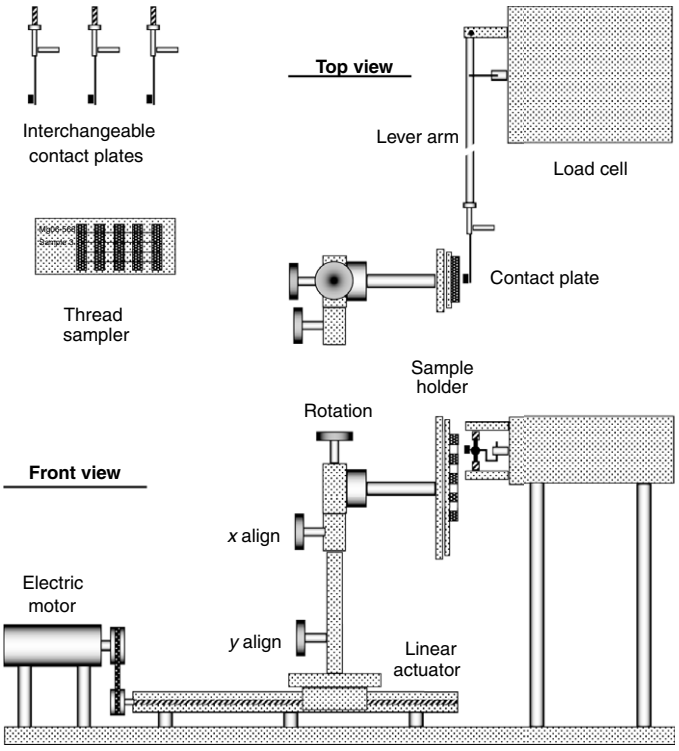

Fig. 3. Thread samplers, the instrument used to measure thread stickiness, and the interchangeable contact plates used with this instrument.

Materials and methods

Species studied and thread collection

We collected threads from newly spun orb-webs constructed by adult females of six Araneoidea species found in Montgomery Co., VA, USA: one species of the family Tetragnathidae, *Leucauge venusta*, and five species of the family Araneidae: *Araneus marmoreus* Clerck, *Araneus pegnia* (Walckenaer), *Argiope trifasciata* (Forskål), *Cyclosa turbinata* (Walckenaer), and *Metepeira labyrinthea* (Hentz). We collected threads on samplers made by gluing raised supports at 4.8 mm intervals to microscope slides (Fig. 3). Double-sided tape on the supports held thread strands securely at their native tension. To ensure that physical and performance characteristics of threads were not affected by changes in environmental conditions, we photographed threads and measured their stickiness within 6.5 h after threads were collected and under the same temperature, percent relative humidity (% RH), and barometric pressure.

Droplet measurements

Before measuring thread stickiness, we made digital images of three thread strands at 50× and two at either 125× (large droplets) or 250× (small droplets). We used Image J (http://www.uhnresearch.ca/facilities/wcif/imagej/) to measure the spacing of a series of droplets in each of the 50× images and the dimensions of three droplets in the 125 or 250× images. The means of these values characterized an individual spider's thread.

Some of the species included in this study had smaller, secondary droplets between the much larger primary droplets (Fig. 1). When secondary droplets were present, their size and distribution were variable. Additionally, secondary droplets comprised only a small percentage of the total droplet volume per mm of capture thread (Table 1). Therefore, we included only primary droplets in this study. We compared the coordinates of the profiles of each species' primary droplets with those generated by equations for parabolas, half-circles, and half-ellipses. Regression analyses showed that droplet coordinates most closely matched those of parabolas (R^2>0.97 for each species). Therefore, we computed droplet volume as two times the integral of the equation of a parabola:

$$y = h[1–(x/b)]^2 ,$$

rotated around the x-axis as follows:

$$V = 2\pi\int_0^b y^2 \mathrm{d}x ,$$

where h=0.5 droplet width and b=0.5 droplet length. This yields the following formula for droplet volume (DV):

$$DV = (2\pi h^2 \times b) / 15 .$$

We computed the spacing of each spider's droplets by

multiplying the mean number of droplets per 1000 μm of thread length by mean droplet length in μm, subtracting this product from 1000 μm, and then dividing the remainder by the number of interdroplet regions in the 1000 μm span (= droplet number – 1).

Stickiness measurements

We measured the stickiness of 12 thread strands per web, three sectors with each of four contact plates having widths of 963, 1230, 1613, and 2133 μm. Prior to beginning each measurement, temperature, barometric pressure and RH were recorded. The mean value registered by each plate was recorded as an individual's stickiness profile. We measured thread stickiness with a smooth acetate plate (Scotch® Magic™ Tape 810 Product Information Sheet, 2002, St Paul, MN, USA) to maximize stickiness and to eliminate the possibility that threads with different droplet profiles might respond differently to a textured surface. We measured each thread with an unused region of the surface and renewed the acetate frequently.

The instrument used to measure stickiness incorporated interchangeable contact plate units attached to the lever arm of a jeweled escapement that transferred force to a load cell machined to increase its sensitivity (Fig. 3). Each interchangeable plate unit consisted of a contact plate fastened to the tip of a small rod that could be threaded into the lever arm of the instrument and secured with a nut. On the back of each unit was a registration pin that extended perpendicular to the face of the contact plate. When a unit was being installed on the lever arm we aligned this pin with a reference jig that was mounted temporarily on the sample holder. This ensured that the face of the contact plate was parallel to the plane of the thread sampler and, therefore, to the threads whose stickiness would be measured. A thread sampler was then attached to the sample holder, which could be moved in three dimensions, permitting a thread strand to be centered on the width of a contact plate and orientated perpendicular to the plate's length before a stickiness measurement was made. After proper thread orientation was achieved, a linear actuator pressed the strand against a contact plate at a speed of 0.06 mm s^{-1} until a force of 25 μN was generated, at which time the direction of travel was immediately reversed. As the thread strand was withdrawn, it exerted force on the plate and the maximum force achieved before the strand pulled free of the plate was recorded as the strand's stickiness.

Statistical and phylogenetic analyses

We used SAS (SAS Institute Inc., Cary, NC, USA) for statistical analyses. To account for phylogenetic relationships among species, we used the PDAP Module (Midford et al., 2005) run under Mesquite (Maddison and Maddison, 2005) to perform independent contrast (IC) analyses (Garland, Jr et al., 1999; Garland, Jr and Ives, 2000; Bloomberg and Garland, Jr, 2002). Relationships among species (Fig. 4) were based on Scharff and Coddington (Scharff and Coddington, 1997). We set all branch lengths to 1, as phylogeny was drastically pruned.

The contribution of individual droplets

To determine if the contribution of droplet adhesion diminishes from edge to center of a thread span, we examined how the increased number of droplets that contacted plates of increasing widths affected the mean per droplet adhesion of a thread span. For each of the four contact plates we performed an IC analysis of the relationship between mean per droplet adhesion and the number of droplets that contacted the plate. To combine the data from the four contact plate widths, we also performed an analysis of the association between the percent change in the number of droplets contacting a plate and the percent change in mean per droplet adhesion. For each of the six species, this produced values for the change between 963 and 1230 μm plates, 1230 and 1613 μm plates, and 1613 and 2133 μm plates. Since each of the three inter-plate percent increases in the number of contacting droplets was the same for the six species, we could not perform an IC analysis on this data and, instead, examined it using standard regression.

Table 1. *Primary droplet dimensions of the six species studied and the environmental conditions under which their thread stickiness was measured*

	Cyclosa turbinata (9)	*Leucauge venusta* (10)	*Metepeira labyrinthea* (8)	*Araneus pegnia* (9)	*Argiope trifasciata* (11)	*Araneus marmoreus* (10)
Spider mass (mg)	7.2±0.9	22.1±3.1	38.0±3.6	65.7±7.1	534.9±86.3	548.3±75.4
Droplets (mm^{-1})	27.51±1.21	31.38±0.99	18.99±1.69	10.05±0.40	6.67±0.28	4.26±0.17
Droplet length (μm)	13.2±1.0	13.8±1.2	23.5±1.9	38.6±3.1	41.5±2.5	67.1±4.5
Droplet width (μm)	9.8±0.8	10.0±0.9	16.4±1.4	28.3±2.4	25.1±1.8	50.2±3.6
Droplet spacing (μm)	26.2±2.9	20.1±1.7	46.6±10.6	72.4±7.8	149.9±24.0	264.2±53.8
Percent secondary droplet volume	10.8±1.7	4.3±1.5	6.4±1.8	0.4±0.1	8.9±2.1	5.4±1.2
Temperature (°C)	22.6±0.1	22.6±0.1	23.5±0.1	23.5±0.1	22.4±0.1	24.1±0.2
% Relative humidity	$32±2^{C}$	$43±1^{A,B}$	$53±0^{A}$	$54±0^{A}$	$38±2^{B,C}$	$51±1^{A}$
Barometric pressure (mmHg)	1016±2	1016±1	1017±1	1017±1	1014±1	1015±1

Values are means ± 1 s.e.m. (*N* values are given in parentheses after species names).
Percent secondary droplet volume is relative to the total droplet volume per mm of capture thread.
For relative humidity, letters denote the ranking (high to low) established by a Ryan–Einot–Gabriel–Welsch Multiple Range Test (P=0.05).

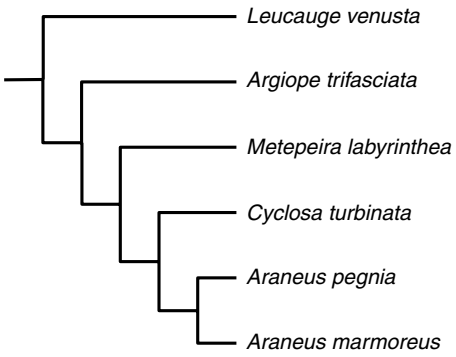

Fig. 4. Relationship of the species included in this study (after Scharff and Coddington, 1997).

Results

Table 1 presents the mean mass of each species, the dimensions of its thread droplets, and the conditions under which thread photographs were taken and thread stickiness was measured. The temperature and barometric pressure under which the six species' measurements were made did not differ (ANOVA, P=0.15 and 0.49, respectively), although RH did (P=0.0001). A Ryan–Einot–Gabriel–Welsch Multiple Range Test ranks these values in Table 1. Fig. 5 compares the mean stickiness, number of droplets per mm, and droplet volume of the six species. These results documented the operation of a SBM, but show that it is affected by droplet size and spacing. An increase in stickiness with increased plate width was observed only in the four species whose threads had the largest, most widely spaced droplets (Fig. 5; two-factor ANOVA: species P<0.0001, plate width P<0.0085). For *L. venusta* and *C. turbinata*, which had the smallest, most closely spaced thread droplets, stickiness differed between species, but not among contact plate widths (species P<0.0001, plate width P>0.93).

The inverse relationship between per-droplet stickiness and the number of droplets in a thread span documented the diminishing adhesive contribution of droplets that are more distant from the edges of thread contact. For each plate width an IC analysis of the stickiness per droplet (dependent variable) and the number of droplets contacting the plate (independent variable) had negative slopes: 963 μm: slope –7.77, two-tailed P=0.0255, R^2=0.75; 1230 μm: slope –4.94, two-tailed P=0.0233, R^2=0.76; 1613 μm: slope –3.77, two-tailed P=0.0237, R^2=0.76; and 2133 μm: slope –2.47, two-tailed P=0.0254, R^2=0.76). When all plate widths were included, a regression of percent change in stickiness per droplet (dependent variable) and percent inter-plate increase in the number of droplets contacting a plate (independent variable) was also negative (Fig. 6; y=–0.556x–1.864, P=0.0003, R^2=0.57). This relationship and the model of thread performance described in the following paragraph explain the failure of plates of increasing widths to register increased stickiness for the threads of *L. venusta* and *C. turbinata* that have small, closely spaced droplets.

We generated an approximate and useful picture of thread performance by assigning stickiness to droplets such that each successive inner droplet contributed half the adhesion of the adjacent outer droplet (Fig. 7). This model shows that only about six droplets at either end of a contacting thread contribute to thread stickiness. Regardless of how much adhesion an individual droplet generates, the length of this approximately 12-droplet maximum efficiency span caps a thread's operational stickiness.

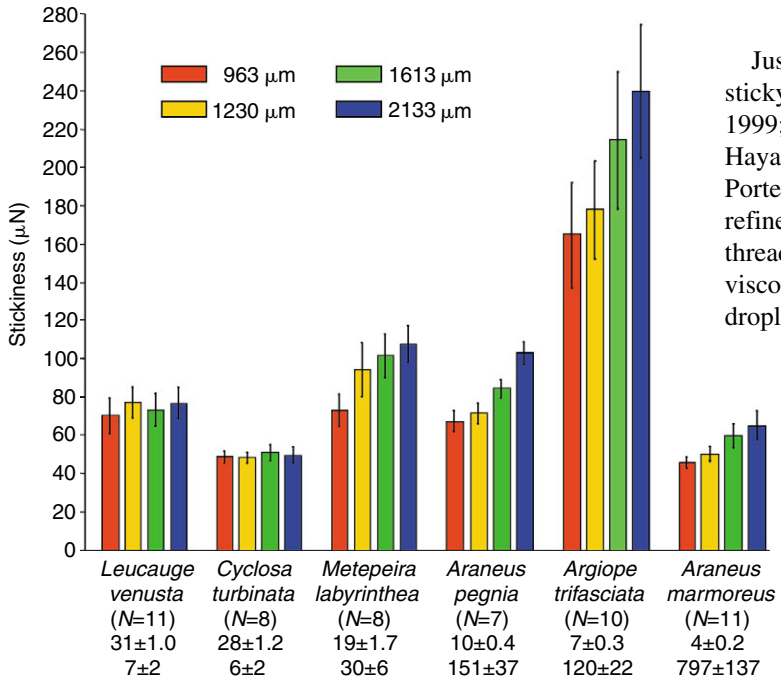

Fig. 5. Stickiness (means ± 1 s.e.m.) measured with four plate widths and, from top to bottom below each genus name, the sample size, number of thread droplets per mm (means ± 1 s.e.m.), and mean droplet volume ($\mu m^3 \times 10^2$ ± 1 s.e.m.).

Discussion

Just as the refined molecular structure of an orb-web's non-sticky thread strengthens the web (Denny, 1976; Gosline et al., 1999; Gosline et al., 2002; Kenney et al., 2002; Craig, 2003; Hayashi et al., 2004; Vollrath and Porter, 2006a; Vollrath and Porter, 2006b), our results show that complementary refinements in the adhesive delivery system of its viscous threads optimizes the web's stickiness. A force that pulls on a viscous thread is distributed effectively over multiple adhesive droplets, reducing the tendency for the thread to peel from a surface, thereby overcoming a limitation of cribellar thread (Hawthorn and Opell, 2003). The effectiveness of SBM appears to be dependent on the plasticity of the thread's droplets and glycoprotein granules and on

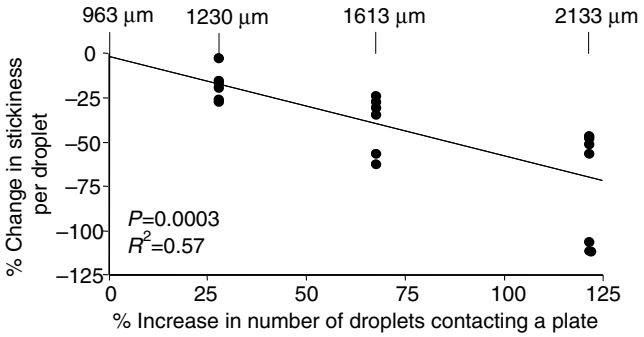

Fig. 6. Relationship between the percent increase in the number of droplets contacting plates of increasing widths and the percent change in the mean droplet adhesion of the longer strands contacting these successively wider plates.

the extensibility of its axial fibers. Our model of adhesive recruitment (Fig. 7) provides a useful, but general picture of the SBM. A more complete portrayal of this mechanism probably needs to account for species-specific differences in both the elasticity of axial fibers and in the plasticity of adhesive droplets and glycoprotein granules.

The SBM explains how droplet profile affects a thread's ability to generate increased stickiness and why threads of *L. venusta* and *C. turbinata* with small, closely spaced droplets failed to register increased stickiness when measured with contact plates of increasing widths. For threads of *L. venusta* with 31.4 droplets mm^{-1}, a maximum efficiency span comprising 12 droplets is approximately 382 µm, only 40% of the narrowest contact plate that we used. Consequently, it is not surprising that these threads failed to register increased stickiness when measured with plates wider than 1000 µm. In contrast, the maximum efficiency span for threads of *A. marmoreus* with 4.3 droplets mm^{-1}, is approximately 2790 µm, indicating that these threads can achieve greater stickiness than we measured.

By attracting atmospheric moisture, the hydrophilic compounds in a viscous thread cause droplet volume to fluctuate with changes in RH (Vollrath et al., 1990; Townley et al., 1991). By photographing and measuring each spider's thread under the same RH we closely linked the physical and performance characteristics of threads. Daily and, in most instances, weekly changes in laboratory RH were small, as indicated by the small standard errors of the mean RH under which each species' threads were measured (Table 1). However, laboratory RH did change seasonally, resulting in threads of *A. marmoreus*, *A. pegnia*, and *M. labyrinthea* being measured around 53% RH, those of *A. trifasciata* and *L. venusta* being measured around 41% RH, and *C. turbinata* being measured at 32% RH. Reduced droplet volume resulting from lower RH may decrease droplet plasticity and reduce the effectiveness of the SBM. However, even at 38% RH *A. trifasciata* threads still exhibited the greatest inter-plate differences in thread stickiness of the six species. Therefore,

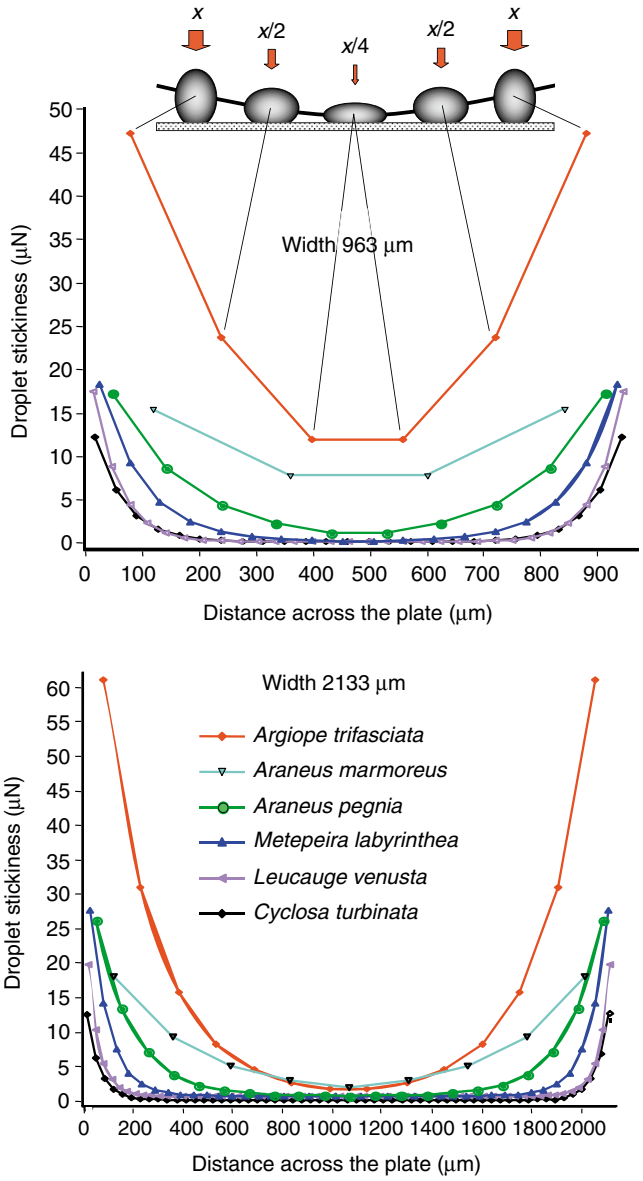

Fig. 7. Models showing the distribution of adhesion among the droplets of six species' threads contacting plates of 930 µm and 2133 µm widths.

the failure of *L. venusta* and *C. turbinata* threads to exhibit inter-plate differences in stickiness cannot be explained entirely by the low RH under which they were measured and must be influenced substantially by their small, closely spaced droplets.

The SBM documented by this study adds a new dimension to the complex issues of orb web architecture, prey interception and profitability (Eberhard, 1986; Eberhard, 1990; Craig, 1987a; Craig, 2003; Wise, 1993), and underscores the important role that spider size plays (Craig, 1987b). Both the volume and spacing of a spider's viscous droplets tend to be directly related to spider size (Opell, 1998; Opell, 2002). Prior our study, it appeared that the close

spacing of droplets produced by small spiders compensated for smaller per droplet adhesion. However, the SBM appears to severely limit the amount of adhesive summation that is possible. This raises the question of why there has apparently been no selection for small spiders to produce larger, more widely spaced droplets, features that would improve the economy of thread adhesion by taking fuller advantage of the SBM. The rate at which a spider's aggregate glands produce or release viscous material probably limits droplet size by determing how much material is available to coalesce into droplets. Thus, selection could more easily favor the production of small, closely spaced droplets by larger spiders, such as *Micrathena gracilis* (Opell, 2002), than of large, more widely spaced droplets by smaller spiders. Evidence for the resource limitation of droplet size comes from the observation that, when starved, *C. turbinata* produce threads with even smaller, more closely spaced droplets (Crews and Opell, 2006).

Small spiders like *C. turbinata* and *L. venusta*, as well as larger spiders like *Micrathena gracilis* (Opell, 2002) that produce threads with small, closely spaced droplets, have closely spaced spirals. This arrangement may partially compensate for the low stickiness of their threads by summing the adhesion of adjacent capture strands that contact an insect. Capture threads with small, closely spaced droplets may be more effective at holding certain surfaces, such as the legs of small insects, or at resisting a force pulling asymmetrically on a thread or pulling parallel to the surface that the thread has contacted. As we measured the adhesion generated by threads that were pulled symmetrically from smooth, flat surfaces, our results do not encompass the range of demands placed on capture threads.

In this study we used a single, smooth surface to measure thread stickiness to facilitate comparisons and modeling. However, the stickiness of viscous threads differs when measured with insect surfaces that have setae of different sizes and densities (B.D.O. and H. S. Schwend, manuscript in preparation). Threads with larger, more widely spaced droplets, like those of *A. trifasciata* and *A. marmoreus*, held insect surfaces more securely than threads with small, closely spaced viscous droplets like *C. turbinata*. However, compared to *A. trifasciata* and *A. marmoreus*, threads of *C. turbinata* registered greater relative stickiness values on fly wings, which are covered by larger setae, and lower relative stickiness on the smooth surfaces of beetle elytra. Thus, an assessment of the prey retention capabilities of an orb web must account for many factors, including capture thread spacing and the insect-surface-specific performance of capture threads.

D. Michael Leonard and Lindsey Neist helped with field and laboratory work. William Alderson helped devise methods for computing droplet volume. A discussion with John Kenney clarified issues related to force distribution in loaded capture threads. Jason Bond and three anonymous reviewers provided useful manuscript suggestions. National Science Foundation grant IOB-0445137 supported this research.

References

Blackledge, T. A. and Hayashi, C. Y. (2006a). Silken toolkits: biomechanics of silk fibers spun by the orb web spider *Argiope argentata* (Fabricius 1775). *J. Exp. Biol.* **209**, 2452-2461.

Blackledge, T. A. and Hayashi, C. Y. (2006b). Unraveling the mechanical properties of composite silk threads spun by cribellate orbweaving spiders. *J. Exp. Biol.* **209**, 3131-3140.

Bloomberg, S. P. and Garland, T., Jr (2002). Tempo and mode in evolution: phenotypic inertia, adaptation and comparative methods. *J. Evol. Biol.* **15**, 899-910.

Bond, J. E. and Opell, B. D. (1998). Testing adaptive radiation and key innovation hypotheses in spiders. *Evolution* **52**, 403-414.

Chacón, P. and Eberhard, W. G. (1980). Factors affecting numbers and kinds of prey caught in artificial spider webs with considerations of how orb-webs trap prey. *Bull. Br. Arachnol. Soc.* **5**, 29-38.

Coddington, J. A. (1986). The monophyletic origin of the orb web. In *Spiders: Webs, Behavior and Evolution* (ed. W. A. Shear), pp. 319-363. Stanford: Stanford University Press.

Coddington, J. A. (1989). Spinneret silk spigot morphology: evidence for the monophyly of orb-weaving spiders, Cyrtophorinae (Araneidae), and the group Theridiidae plus Nesticidae. *J. Arachnol.* **17**, 71-96.

Craig, C. L. (1987a). The ecological and evolutionary interdependence between web architecture and web silk spun by orb web weaving spiders. *Biol. J. Linn. Soc. Lond.* **30**, 135-162.

Craig, C. L. (1987b). The significance of spider size in the diversification of spider-web architecture and spider reproductive modes. *Am. Nat.* **129**, 47-68.

Craig, C. L. (2003). *Spider Webs and Silk: Tracing Evolution from Molecules to Genes to Phenotypes*. New York: Oxford University Press.

Craig, C. L. and Bernard, G. D. (1990). Insect attraction to ultraviolet-reflecting spider webs and web decorations. *Ecology* **71**, 616-624.

Craig, C. L., Bernard, G. D. and Coddington, J. (1994). Evolutionary shifts in the spectra properties of spider silks. *Evolution* **48**, 287-296.

Crews, S. E. and Opell, B. D. (2006). The features of capture threads and orb-webs produced by unfed *Cyclosa turbinata* (Araneae: Araneidae). *J. Arachnol.* **34**, In Press.

Denny, M. (1976). Physical properties of spider silks and their role in design of orb-webs. *J. Exp. Biol.* **65**, 483-506.

Eberhard, W. G. (1986). Effect of orb-web geometry on prey interception and retention. In *Spiders: Webs, Behavior, and Evolution* (ed. W. A. Shear), pp. 70-100. Stanford: Stanford University Press.

Eberhard, W. G. (1989). Effects of orb-web orientation and spider size on prey retention. *Bull. Br. Arachnol. Soc.* **8**, 45-48.

Eberhard, W. G. (1990). Function and phylogeny of spider webs. *Annu. Rev. Ecol. Syst.* **21**, 341-372.

Foelix, R. F. (1996). *Biology of Spiders* (2nd edn). New York: Oxford University Press.

Garb, J. E., DiMauro, T., Vo, V. and Hayashi, C. Y. (2006). Silk genes support the single origin of orb webs. *Science* **312**, 1762.

Garland, T., Jr and Ives, A. R. (2000). Using the past to predict the present: confidence intervals for regression equations in phylogenetic comparative methods. *Am. Nat.* **155**, 346-364.

Garland, T., Jr, Midford, P. E. and Ives, A. R. (1999). An introduction to phylogenetically based statistical methods, with a new method for confidence intervals on ancestral values. *Am. Zool.* **39**, 374-388.

Gosline, J. M., Denny, M. W. and Demont, M. E. (1984). Spider silk as rubber. *Nature* **309**, 551-552.

Gosline, J. M., Cuerette, P. A., Ortlepp, C. S. and Savage, K. N. (1999). The mechanical design of spider silks: from fibroin sequence to mechanical function. *J. Exp. Biol.* **202**, 3295-3303.

Gosline, J., Lillie, M., Carrington, E., Guerette, P., Ortlepp, C. and Savage, K. (2002). Elastic proteins: biological roles and mechanical properties. *Philos. Trans. R. Soc. Lond. B Biol. Sci.* **357**, 121-132.

Griswold, C. E., Coddington, J. A., Hormiga, G. and Scharff, N. (1998). Phylogeny of the orb-web building spiders (Araneae, Orbiculariae: Deinopoidea, Araneoidea). *Zool. J. Linn. Soc.* **123**, 1-99.

Guerette, P. A., Ginzinger, D. G., Weber, B. H. F. and Gosline, J. M. (1996). Silk properties determined by gland-specific expression of a spider fibroin gene family. *Science* **272**, 112-114.

Hawthorn, A. C. and Opell, B. D. (2002). Evolution of adhesive mechanisms in cribellar spider capture thread: evidence for van der Waals and hygroscopic forces. *Biol. J. Linn. Soc. Lond.* **77**, 1-8.

Hawthorn, A. and Opell, B. D. (2003). van der Waals and hygroscopic forces

of adhesion generated by spider capture threads. *J. Exp. Biol.* **206**, 3905-3911.

Hayashi, C. and Lewis, R. V. (2000). Molecular architecture and the evolution of a modular spider silk protein gene. *Science* **287**, 1477-1479.

Hayashi, C. Y., Blackledge, T. A. and Lewis, R. V. (2004). Molecular and mechanical characterization of aciniform silk: uniformity of iterated sequence modules in a novel member of the spider silk fibroin gene family. *Mol. Biol. Evol.* **21**, 1950-1959.

Kenney, J. M., Knight, D., Wise, M. J. and Vollrath, F. (2002). Amyloidogenic nature of spider silk. *Eur. J. Biochem.* **269**, 4159-4163.

Maddison, W. P. and Maddison, D. R. (2005). Mesquite: a modular system for evolutionary analysis. Version 1.06 http://mesquiteproject.org.

Midford, P. E., Garland, T., Jr and Maddison, W. (2005). PDAP:PDTREE package for Mesquite, version 1.07. http://mesquiteproject.org/pdap_mesquite/.

Opell, B. D. (1994a). Factors governing the stickiness of cribellar prey capture threads in the spider family Uloboridae. *J. Morphol.* **221**, 111-119.

Opell, B. D. (1994b). The ability of spider cribellar prey capture thread to hold insects with different surface features. *Funct. Ecol.* **8**, 145-150.

Opell, B. D. (1997a). Changes in spinning anatomy and thread stickiness associated with the origin of orb-weaving spiders. *Biol. J. Linn. Soc. Lond.* **62**, 443-458.

Opell, B. D. (1997b). The material cost and stickiness of capture threads and the evolution of orb-weaving spiders. *Biol. J. Linn. Soc. Lond.* **62**, 443-458.

Opell, B. D. (1998). Economics of spider orb-webs: the benefits of producing adhesive capture thread and of recycling silk. *Funct. Ecol.* **12**, 613-624.

Opell, B. D. (1999). Redesigning spider webs: stickiness, capture area, and the evolution of modern orb-webs. *Evol. Ecol. Res.* **1**, 503-516.

Opell, B. D. (2002). Estimating the stickiness of individual adhesive capture threads in spider orb webs. *J. Arachnol.* **30**, 494-502.

Opell, B. D. and Bond, J. E. (2000). Extensibilities of cribellar and adhesive capture threads of orb-weaving spiders: testing punctuated and associative explanations of character evolution. *Biol. J. Linn. Soc. Lond.* **70**, 107-120.

Opell, B. D. and Bond, J. E. (2001). Changes in the mechanical properties of capture threads and the evolution of modern orb-weaving spiders. *Evol. Ecol. Res.* **3**, 567-581.

Peñalver, E., Grimaldi, D. A. and Delclòs, X. (2006). Early cretaceous spider web with its prey. *Science* **312**, 1761.

Peters, H. M. (1984). The spinning apparatus of Uloboridae in relation to the structure and construction of capture threads (Arachnida, Araneida). *Zoomorphology* **104**, 96-104.

Peters, H. M. (1986). Fine structure and function of capture threads. In *Ecophysiology of Spiders* (ed. W. Nentwig), pp. 187-202. New York: Springer Verlag.

Peters, H. M. (1995). Ultrastructure of orb spiders' gluey capture threads. *Naturwissenschenschaften* **82**, 380-382.

Platnick, N. I. (2006). *The World Spider Catalog, V7.0* (ed. P. Merrett and H. D. Cameron), http://research.amnh.org/entomology/spiders/catalog/INTRO1.html. New York: The American Museum of Natural History.

Scharff, N. and Coddington, J. A. (1997). A phylogenetic analysis of the orb-weaving spider family Araneidae (Arachnida, Araneae). *Zool. J. Linn. Soc.* **120**, 355-434.

Selden, P. A. (1989). Orb-web weaving spiders in the early Cretaceous. *Nature* **340**, 711-713.

Townley, M. A. (1990). Compounds in the droplets of the orb spider's viscid spiral. *Nature* **345**, 526-528.

Townley, M. A., Bernstein, D. T., Gallagher, K. S. and Tillinghast, E. K. (1991). Comparative study of orb web hygroscopicity and adhesive spiral composition in three araneid spiders. *J. Exp. Zool.* **259**, 154-165.

Vollrath, F. and Porter, D. (2006a). Spider silk as a model biomaterial. *Appl. Phys. A* **82**, 205-212.

Vollrath, F. and Porter, D. (2006b). Spider silk as archetypal protein elastomer. *Soft Matter* **2**, 377-385.

Vollrath, F. and Tillinghast, E. K. (1991). Glycoprotein glue beneath a spider web's aqueous coat. *Naturwissenschaften* **78**, 557-559.

Vollrath, F., Fairbrother, W. J., Williams, R. J. P., Tillinghast, E. K., Bernstein, D. T., Gallagher, K. S. and Townley, M. A. (1990). Compounds in the droplets of the orb spider's viscid spiral. *Nature* **345**, 526-528.

Wise, D. H. (1993). *Spiders in Ecological Webs*. New York: Cambridge University Press.

Zschokke, S. (2002). Ultraviolet reflectance of spiders and their webs. *J. Arachnol*. **30**, 246-254.